Two-Dimensional Graphene Superlattice: Energy Spectrum and Current-Voltage Characteristics

S.V. Kryuchkov[1,2,*], C.A. Popov[1,†]

[1] *Volgograd State Socio-Pedagogical University, Physical Laboratory of Low-Dimensional Systems, 27, Lenin Ave., 400066 Volgograd, Russia*

[2] *Volgograd State Technical University, 28, Lenin Ave. 400005 Volgograd, Russia*

The properties of two-dimensional graphene-based superlattice are studied. The creation of a two-dimensional periodic potential in the graphene layer is assumed to be alternating in a checkerboard pattern of rectangular areas of the substrate materials. For this system the energy spectrum and an expression for the current in the graphene layer were obtained. The influence of a transverse constant electric field on the current is investigated. It is shown that the presence of the transverse field leads to the appearance of an additional peak in the current-voltage characteristics of the superlattice.

Keywords: Graphene, Two-dimensional superlattice, Energy spectrum, Current-voltage characteristics, Constant electric field.

1. INTRODUCTION

Recent years were marked by increased researcher's interest to graphene and materials on its basis [1-3]. Theoretically and experimentally electronic structure, transport properties, electronic, optical and other phenomena were studied.

But unique properties of pure graphene can be modified. One of the modification variants is a constructing of the superlattice – a structure with additional periodic potential.

A number of methods of graphene-based superlattice construction were proposed and realized. For example, in graphene superlattices consisting of monolayer or bilayer graphene the transport properties of charge carriers were studied in Ref. [4]. The conductance of disordered graphene superlattices was investigated in [5]. In this case, the superlattice was consisted of different type-doped graphene of various thicknesses.

A number of electronic properties of graphene/hexagonal boron nitride (*h*-BN) superlattices were explored in [6, 7].

Graphene superlattice can be realized by putting a series of magnetic insulator bars on top of a graphene sheet [8]. Also graphene properties can be modulated by magnetic field [9].

In Ref. [10] it was proposed the two-dimensional superlattice made with partial hydrogenation of graphene.

In this article we study energy spectrum and current-voltage characteristics of the graphene superlattice with substrate consists of alternate in a checkerboard pattern areas of SiO₂/SiC or SiO₂/*h*-BN (Fig. 1).

As it was shown [11] the substrate SiO₂/*h*-BN is more perspective for using with the graphene sheet. This is due to the fact that graphene and *h*-BN have a similar hexagonal structure. And sizes of their lattices differ just for 2 %.
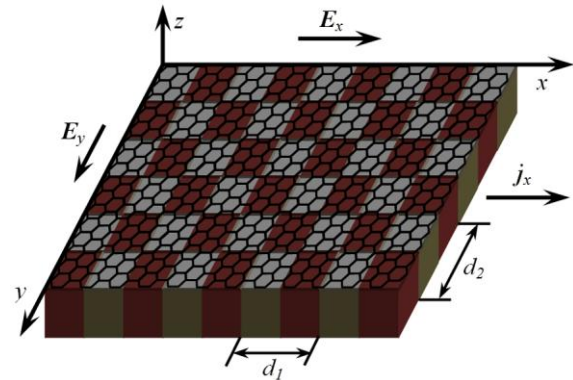
Fig. 1 – Geometry of the substrate location relative to the graphene sheet

These alternate regions create in the graphene sheet periodic structure with a period of d_1 along one axis (the *x*-axis, in this case) and the period of d_2 along the *y*-axis.

2. ENERGY SPECTRUM OF TWO-DIMENSIONAL GRAPHENE-BASED SUPERLATTICE

In this case the wave function for the electron is the spinor function

$$\psi(\vec{r}) = \begin{pmatrix} \psi_1(\vec{r}) \\ \psi_2(\vec{r}) \end{pmatrix}, \tag{1}$$

where functions $\psi_1(\vec{r})$ and $\psi_2(\vec{r})$ describe electron states in different graphene sublattices.

$$\psi(\vec{r}) = \sum_m \sum_n \exp(ink_x d_1 + imk_y d_2)\varphi_{nm}(\vec{r}) \tag{2}$$

Function $\varphi_{nm}(\vec{r})$ is a spinor function that is not de-

pend on the shifting along the x-axis on the vector $\vec{d}_1$ and along the y-axis on the vector $\vec{d}_2$. Then we have

$$\varphi_{nm}(\vec{r}) = \begin{pmatrix} \xi_1(\vec{r} + n\vec{d}_1 + m\vec{d}_2) \\ \xi_2(\vec{r} + n\vec{d}_1 + m\vec{d}_2) \end{pmatrix}. \tag{3}$$

To describe the electron state in the superlattice the Dirac equation can be written as

$$\upsilon_F(\hat{\sigma}_x \hat{p}_x + \hat{\sigma}_y \hat{p}_y)\psi + \hat{\sigma}_z U(\vec{r})\psi = \varepsilon\psi. \tag{4}$$

Here $\hat{\sigma}_x$, $\hat{\sigma}_x$, $\hat{\sigma}_x$ are the Pauli matrices, υ_F is the Fermi velocity, $U(\vec{r})$ is two-dimensional periodic potential, and the momentum operator $\hat{p} = -i\nabla$ (in terms of $\hbar = 1$).

Equation (4) in a matrix form

$$\hat{M}\psi = \varepsilon\psi, \tag{5}$$

where $\hat{M} = \begin{pmatrix} U(\vec{r}) & \upsilon_F\left(-i\dfrac{\partial}{\partial x} - \dfrac{\partial}{\partial y}\right) \\ \upsilon_F\left(-i\dfrac{\partial}{\partial x} + \dfrac{\partial}{\partial y}\right) & -U(\vec{r}) \end{pmatrix}.$

Multiplying Eq. (5) by $\hat{M}$ on the left (using the procedure [12]), we obtain

$$\hat{M}^2\psi = \hat{M}\varepsilon\psi$$

or

$$\hat{M}^2\psi = \varepsilon^2\psi. \tag{6}$$

$\hat{M}^2$ is a diagonal matrix. This allows us to form equations for the spinor (1) components. The equation for the first component

$$\left[U^2(\vec{r}) - \upsilon_F^2\left(\frac{\partial^2}{\partial x^2} + \frac{\partial^2}{\partial y^2}\right)\right]\psi_1 = \varepsilon^2\psi_1. \tag{7}$$

As a result of multiplication by the complex conjugate function, we have

$$\varepsilon^2 = \frac{\int \psi_1^*\left[U^2(\vec{r}) - \upsilon_F^2\left(\dfrac{\partial^2}{\partial x^2} + \dfrac{\partial^2}{\partial y^2}\right)\right]\psi_1 d\vec{r}}{\int \psi_1^*\psi_1 d\vec{r}},$$

or

$$\varepsilon^2 = \frac{\int \psi_1^* U^2(\vec{r})\psi_1 d\vec{r}}{\int \psi_1^*\psi_1 d\vec{r}} - \frac{\int \psi_1^* \upsilon_F^2\left(\dfrac{\partial^2}{\partial x^2} + \dfrac{\partial^2}{\partial y^2}\right)\psi_1 d\vec{r}}{\int \psi_1^*\psi_1 d\vec{r}}. \tag{8}$$

To find the value of the second item we consider the electron state in the well with numbers (n, m). For the electron state in the internal region of the well the Dirac equation can be written as

$$\upsilon_F(\hat{\sigma}_x \hat{p}_x + \hat{\sigma}_y \hat{p}_y)\varphi_{nm} = \varepsilon_0\varphi_{nm}. \tag{9}$$

Here ε_0 is the energy of the electron motion as if it was located in this well. Following the same procedure we obtain the expression

$$-\upsilon_F^2\left(\frac{\partial^2}{\partial x^2} + \frac{\partial^2}{\partial y^2}\right)\varphi_{nm} = \varepsilon_0^2\varphi_{nm}. \tag{10}$$

After integration and substitution into the Eq. (8) we have

$$\varepsilon^2 = \varepsilon_0^2 + \frac{\int \psi_1^* U^2(\vec{r})\psi_1 d\vec{r}}{\int \psi_1^*\psi_1 d\vec{r}}. \tag{11}$$

Some transformations lead us to the electron energy spectrum in approximation of nearest neighbors

$$\varepsilon^2 = \varepsilon_0^2 + \frac{W_{00} + 4W_{10}\cos(k_x d_1) + 4W_{01}\cos(k_y d_2)}{1 + 4S_{10}\cos(k_x d_1) + 4S_{01}\cos(k_y d_2)}. \tag{12}$$

Here

$$W_{nm} = \int \xi_1(\vec{r} + n\vec{d}_1 + m\vec{d}_2)U^2(\vec{r})\xi_1(\vec{r})d\vec{r},$$

$$S_{nm} = \int \xi_1(\vec{r} + n\vec{d}_1 + m\vec{d}_2)\xi_1(\vec{r})d\vec{r},$$

Simplifying Eq. (12) we obtain the energy spectrum in the following form

$$\varepsilon = \pm\sqrt{\Delta^2 + \Delta_1^2\left(1 - \cos(k_x d_1)\right) + \Delta_2^2\left(1 - \cos(k_y d_2)\right)} \tag{13}$$

where $\quad \Delta^2 = \varepsilon_0^2 + W_{00} + 4\left(W_{10} + W_{01} - W_{00}(S_{10} + S_{01})\right),$
$\Delta_1^2 = 4\left(W_{00}S_{10} - W_{10}\right),\quad \Delta_2^2 = 4\left(W_{00}S_{01} - W_{01}\right).$

This spectrum is non-additive. This fact means that any connected with spectrum impact applied along the one of axis should influence the process along another axis.

3. CURRENT-VOLTAGE CHARACTERISTICS

Now we consider the effect of the constant electric field $\vec{E}(E_x, E_y, 0)$ on the graphene superlattice, supposing that electric current flows in the x-axis direction (see Fig. 1).

The current density in the two-dimensional graphene sheet is given by

$$j_x = \frac{2e}{(2\pi)^2}\int_{\vec{p}} \upsilon_x(\vec{p})f(\vec{p}, t)d\vec{p}, \tag{14}$$

where the electron velocity is the momentum derivative of the energy (13) (in the Eq. (13) we can substitute $k_x = p_x$ and $k_y = p_y$ because earlier we putted $\hbar = 1$) and the distribution function $f(\vec{p}, t)$ is the solution of the Boltzmann equation

$$\frac{\partial f}{\partial t} + e\vec{E}\,\frac{\partial f}{\partial \vec{p}} = -\nu\big(f(\vec{p}) - f_0(\vec{p})\big). \qquad (15)$$

The right part of this equation is taken in approximation of the constant frequency of interactions ν. $f(\vec{p})$ and $f_0(\vec{p})$ are nonequilibrium and equilibrium distribution functions respectively. The solution of (15) can be written as

$$f(\vec{p}) = \nu \int_{-\infty}^{t} dt' \exp\big(-\nu(t-t')\big) f_0\big(\vec{p}\,'(t',\vec{p},t)\big), \quad (16)$$

where $\vec{p}\,'$

$$\frac{d\vec{p}\,'}{dt} = e\vec{E} \qquad (17)$$

with initial conditions $\vec{p}\,' = \vec{p}$, $t' = t$, and equilibrium

distribution function is determined as

$$f_0(\vec{p}) = C \cdot \exp\left(-\frac{\varepsilon(\vec{p})}{kT}\right). \qquad (18)$$
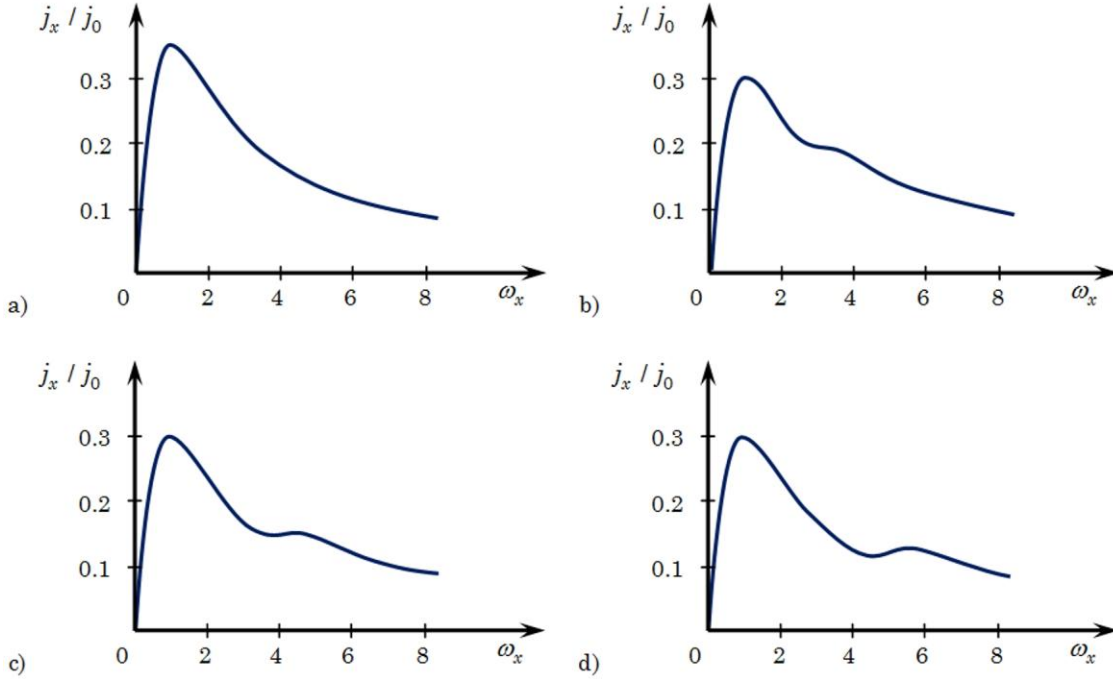
Here C is a normalization constant that has the value

$$C = \frac{n_0 d_1 d_2}{2 a_0} \exp\left(\frac{D}{kT}\right), \qquad (19)$$

where a_0 is the graphene sheet width, n_0 is the surface concentration of the charge carries, $D = \sqrt{\Delta^2 + \Delta_1^2 + \Delta_2^2}$.

We obtain an expression for the velocity of the electron motion along the x-axis. Then this expression and Eq. (17) and (18) are substituted to the Eq. (14). The current density can be written using dimensionless parameters in the integral as follows

$$j_x = j_0 \int_0^{\infty} d\tau \exp(-\tau) \int_{-\pi}^{\pi}\int_{-\pi}^{\pi} d\alpha\, d\beta\, \frac{\sin\alpha \cdot \exp\left(-\dfrac{D}{kT}\sqrt{1 - \dfrac{\Delta_1^2}{D^2}\cos(\alpha + \omega_x\tau) - \dfrac{\Delta_2^2}{D^2}\cos(\beta + \omega_y\tau)}\right)}{\sqrt{1 - \dfrac{\Delta_1^2}{D^2}\cos\alpha - \dfrac{\Delta_2^2}{D^2}\cos\beta}}. \qquad (20)$$

Fig. 2 – Graphs of the current density depending on the value of ω_x for different values of ω_y : a) $\omega_y = 0$, b) $\omega_y = 3$, c) $\omega_y = 4$, d) $\omega_y = 5$.

Here $\omega_x = \dfrac{e E_x d_1}{\nu}$ and $\omega_y = \dfrac{e E_y d_2}{\nu}$ are dimensionless frequencies, and

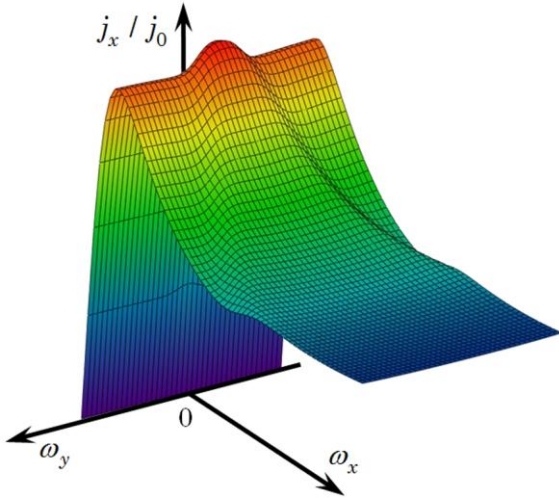$$j_0 = \frac{e \Delta_1^2 d_1 n_0 \exp\left(\dfrac{D}{kT}\right)}{8\pi^2 a_0 D}.$$

The expression (20) can be studied analytically and numerically.

Results of the numerical analysis are presented on the Fig. 2. Numerical analysis of Eq. (20) shows that in the presence of the transverse electric field component, an additional maximum appears on the current-voltage characteristic slightly shifted from the value of ω_y in

the direction of a strong field.

Presented by Eq. (20) function can't be integrated exactly. Using conditions $\Delta_1 / D < 1$ and $\Delta_2 / D < 1$ allows us to approximate exponent function in (20) as a polynomial of degree two:

$$j_x = \frac{|e|\Delta_1^4 d_1 n_0}{8kTa_0 D^2}\left(\frac{\omega_x}{\omega_x^2+1} + \frac{D/kT+1}{16} \cdot \left[\frac{\Delta_1^2}{D^2} \cdot \frac{\omega_x}{4\omega_x^2+1} + \frac{\Delta_2^4}{D^4} \cdot \frac{\omega_x - \omega_y}{\left(\omega_x - \omega_y\right)^2+1} + \frac{\Delta_2^4}{D^4} \cdot \frac{\omega_x + \omega_y}{\left(\omega_x + \omega_y\right)^2+1} \right] \right). \tag{21}$$

Fig. 3 – 3-d graph of current density constructed according to (21) with the range of values: ω_x from 0 to 8 and ω_y from – 6 to 6

It is easy to notice from the Fig. 3 that the appearance of even a small field along the *y*-axis leads to the decrease in the main current density maximum. Further increase of the E_y leads to the stabilization of the current density value.

$$\exp\left(-\gamma\sqrt{1-x}\right) \approx \exp(-\gamma)\left(1 + \frac{\gamma}{2}x + \frac{\gamma(\gamma+1)}{8}x^2\right).$$

The same degree of the root representation and integration leads to the following expression for current density:

4. CONCLUSION

Energy spectrum of the graphene-based superlattice was studied in the framework of nearest neighbors. It was shown that the superlattice spectrum keeps the basic features of graphene spectrum but depends on the superlattice parameters. Its non-additive character shows possibility of mutual effect of processes proceeding in the perpendicular directions.

Using obtained spectrum the expression for the current density was found. Analytical and numerical analysis shows the effect of the crosscurrent constant electric field leads to the appearance of the additional maximum of the current density and decrease of the maximal value of the current.

AKNOWLEDGEMENTS

REFERENCES

1. A.K. Geim, K.S. Novoselov, *Nat. Mater.* **6**, 184 (2007).
2. K.S. Novoselov, A.K. Geim, S.V. Morozov, D. Jiang, Y. Zhang, S.V. Dubonos, I.V. Grigorieva, A.A. Firsov, *Science* **306**, 666 (2004).
3. S. Stankovich, D.A. Dikin, G.H.B. Dommett, K.M. Kohlhaas, E.J. Zimney, E.A. Stach, R.D. Piner, S.T. Nguyen, R.S. Ruoff, *Nature* **442**, 282 (2006).
4. C. Bai, X. Zhang, *Phys. Rev. B* **76**, 075430 (2007).
5. N. Abedpour, A. Esmailpour, R. Asgari, M.R.R. Tabar, *Phys. Rev. B* **79**, 165412 (2009).
6. R.V. Gorbachev, J.C.W. Song, G.L. Yu, A.V. Kretinin, F. Withers, Y. Cao, A. Mishchenko, I.V. Grigorieva, K.S. Novoselov, L.S. Levitov, A.K. Geim, *Science* **346**, 448 (2014).
7. P. Moon, M. Koshino, *Phys. Rev. B* **90**, 155406 (2014).
8. Z.P. Niu, F.X. Li, B.G. Wang, L. Sheng, D.Y. Xing, *Eur. Phys. J. B* **66**, 245 (2008).
9. Y.-X. Li, *J. Phys.-Condens. Mat.* **22**, 015302 (2010).
10. M. Yang, A. Nurbawono, C. Zhang, Y.P. Feng, Ariando, *Appl. Phys. Lett.* **96**, 193115 (2010).
11. P.V. Ratnikov, *JETP Lett.* **90**, 469 (2009).
12. S.V. Kryuchkov, E.I. Kukhar', *Physica B* **408**, 188 (2013).